Evolution and interaction of LD slag as an oxygen carrier in a 12 MW_{th} boiler

Fredrik HILDOR[1]*, Tobias MATTISSON[2], Henrik LEION[1], Carl Johan LINDERHOLM[2], Magnus RYDÉN[2]

[1] *Chemistry and Chemical Engineering, Chalmers University of Technology, 412 93 Göteborg, Sweden*

[2] *Department of Space, Earth and Environment, Chalmers University of Technology, 412 93 Göteborg, Sweden*

**Corresponding Author, fredrik.hildor@chalmers.se,*

Abstract

LD slag is a byproduct originating from the basic oxygen steel production process in which raw iron from the blast furnace is converted to steel. LD slag contains mainly calcium and iron compounds and a smaller amount of magnesium, silicon, manganese and vanadium. The iron content, about 17 wt.% of the slag, makes this material a potential oxygen carrier for combustion processes such as Oxygen Carrier Aided Combustion (OCAC) or Chemical Looping Combustion (CLC). A fraction of the LD slag produced can be recirculated to the blast furnace as slag former, but there is limited external demand for the remaining material. This study will present an investigation of the use of LD slag as an oxygen carrier in OCAC at semi-industrial scale. The Chalmers 12 MW_{th} biomass circulating fluidized bed boiler was operated using LD slag as bed material under OCAC conditions during a period of two weeks. During the operation, bed samples from the boiler were extracted and analyzed with ICP-SFMS, SEM-EDS, XRD and different mechanical tests to analyze the chemical and physical changes of the bed material as a function of time. The samples were also investigated in a laboratory fluidized bed reactor to determine the material's change in reactivity towards common volatile fuel components, i.e. CO, H_2, CH_4 and C_6H_6. It was found that LD slag can be utilized as an oxygen carrier in a combustion process for biofuel. However, the reactivity towards syngas, methane and benzene is reduced as a function of time in the boiler, this is believed to be caused by accumulation and interaction of alkali form the biofuel ash. Sulfur addition may decrease the negative effects of alkali on combustion efficiency, but not eradicate them completely.

Keywords

LD slag, Oxygen Carrier, Oxygen Carrier Aided Combustion, Chemical Looping Combustion, Recycling, Ash interaction, Ash

Introduction and Background

Climate change due to human activity is now widely accepted knowledge and supported by fundamental science. It is also known that climate change is damaging for humans and our society, which is why climate change should be mitigated to increase our resilience space – our ability to withstand stresses. Emissions of carbon dioxide from combustion of fossil fuels is the main contributor of greenhouse gases. To mitigate the carbon dioxide emissions, or even remove carbon dioxide from the atmosphere, increased energy effectivity and Carbon Capture and Storage can be applied to point emission sources[1]. To increase energy efficiency on point emission sources, based on fluidized bed combustion technologies, active bed materials can be used. Active bed materials such as oxygen carriers, commonly transition metal oxides, can be applied to improve the performance and reduce emissions; this approach is normally called Oxygen Carrier Aided Combustion (OCAC)[2]. The oxygen carrier transports both heat and oxygen to locations in the bed where the oxygen is released to oxidize the fuel[2]. Another technology that can be used to separate carbon dioxide called, normally Chemical Looping Combustion (CLC), also utilize oxygen carriers to transport oxygen from an air reactor to the fuel in a fuel reactor[3]. The choice of oxygen carriers is of great concern when evaluating and designing a plant since different oxygen carriers have different properties regarding e.g. fuel conversion, oxygen transport limitations, reactivity and selectivity[3–5].

Low-cost oxygen carriers for CLC and OCAC are highly interesting when solid fuel is used. The reason for this is that solid fuels have a high ash content that is both corrosive, especially for biomass ash[6], and contains alkali that may contribute to agglomeration and deactivation of oxygen carriers[3,7]. Guidelines to find suitable oxygen carriers for solid fuel combustion include[8–10]:

- Sufficient reactivity towards both oxygen and fuel,
- High enough reduction potential to be able to transport a significant amount of oxygen,
- High melting temperature to avoid sintering,
- Low harmful impact on the environment; before, during and after use as an oxygen carrier,
- Sufficient mechanical strength to limit attrition,
- The material should be obtainable at a low cost.

Generally, the transition metals Fe, Mn, Ni, Cu and Co could be used as oxygen carriers[11]. However, when contemplating the guidelines for oxygen carriers for solid fuels mainly iron and manganese-based materials are of interest since Ni and Co could have harmful impact on the environment and Cu has been shown to have agglomeration issues[3,9,12]. Iron-based oxygen carriers for solid fuel CLC are particularly interesting due to their relatively low cost and non-harmful nature. Iron-based oxygen carriers could be obtained in different ways, from synthetically produced particles[11] to different iron ores and industrial waste products, such as slags, oxidation scales and sewage sludge ash[13–15]

LD-Slag

LD-slag, LD-stone or Basic Oxygen Furnace (BOF) slag is a by-product from the basic oxygen steel production process, also called Linz–Donawitz process. In this process, iron is converted to steel by the addition of fluxes, alloying additives and scraps under oxidative environment[16]. About 85-165 kg LD-slag is produced for every ton of produced steel[16], but the amount can be up to 200 kg/ton steel[17]. The major elements in LD-slag is CaO (30-60%), FeO (10-35%) and SiO_2 (8-20%)[16,18,19]. Depending on the origin of the iron ore, other elements such as Mg, Mn, Al, Ti, V could contribute to a significant amount to the slag composition[18,19].

LD-slag can be utilized in different applications such as road construction material, hydraulic engineering and fertilizer as well as internally in the ironmaking process to a certain amount. The amount of iron and calcium recycled within the ironmaking process is however limited due to the high amount of phosphorus in the slag. Unfortunately, although several efforts have been committed the last years a large amount of the LD-slag is still landfilled or stored for later applications[16,17,20]. In the Nordic region, the landfilling is implemented to a significant degree since the vanadium concentration is high[20]. Due to the high Vanadium concentration, the LD-slag utilization as fertilizer has been limited since vanadium is a heavy metal soil pollutant[21].

Since LD-slag is available and cheap and has a relatively high concentration of iron, it has been of interest as an oxygen carrier for chemical looping applications[22–24]. Also, since the calcium content in LD-slag is high, it could be expected that it has good catalytic properties for the water-gas-shift reaction at temperatures around 950°C, which could have a substantial effect inside the fuel reactor in CLC. CaO is namely a well-known catalyst for the water-gas shift reaction at high temperatures[25]. This means that the production of highly reactive H2 could be increased, which may promote the overall reactivity. So far, the main findings of LD slag as an oxygen carrier are that it has a limited hydrocarbon conversion[22,23] but a relatively good CO conversion[24]. Previous studies have been performed in small scale laboratory batch reactors. In the current project, LD-slag was used as an oxygen carrier in OCAC at semi-industrial scale. The material replaced sand in the Chalmers 12MW_{th} fluidized bed boiler and was operated over 90 h. The aim of this particular study was to investigate LD slag as an oxygen carrier and the material behavior as an effect of this operational time from a physical and chemical perspective.

Experimental section

Material and Procedure

The LD-slag was received from SSAB MEROX, Sweden. Around 28 metric ton material in the size fraction between 150-400µm was sieved and transported to Chalmers 12MW_{th} circulating fluidized bed (CFB) boiler. Layout of the boiler can be seen in Figure 1 and further information regarding the boiler dimensions can be found elsewere[2]. The material was used as an active bed material in the boiler operated with biomass as fuel the under OCAC conditions[2], during two weeks of operation. During the first week, LD slag was operated continuously with no addition of any other bed material, i.e. 24 h a day. No bed material was extracted, but more material was inserted as bed pressure was lost due to material loss in the primary cyclone and dehydrogenation of calcium hydroxide originating from the LD slag. The boiler was operated around 860°C using wood-chips as fuel as a normal CFB boiler with the exception of LD slag being used as bed material instead of sand.

Bed material was extracted from the lower part of the furnace during operation of the boiler. This was done via a cooled collection probe. Roughly 1 kg of material was extracted at least two times a day during the first week of operation. Four samples were chosen for closer analysis for this paper; each one of them collected in the morning when the process parameters had been stable during the night. During the night operation, the fuel addition was constant at 1600-1700kg/h and the primary air flow set to 1.4-1.5 kg/s resulting in a temperature of 850-860°C. The total bed inventory was about 2000 kg of LD slag. Another sample was also chosen from the fourth day of operation when elementary sulfur had been added to the furnace to investigate effects on CO conversion. These samples were compared with fresh material, from the same batch, that had been oxidized at 950°C for 24 h to remove water and transform unstable crystal structures.

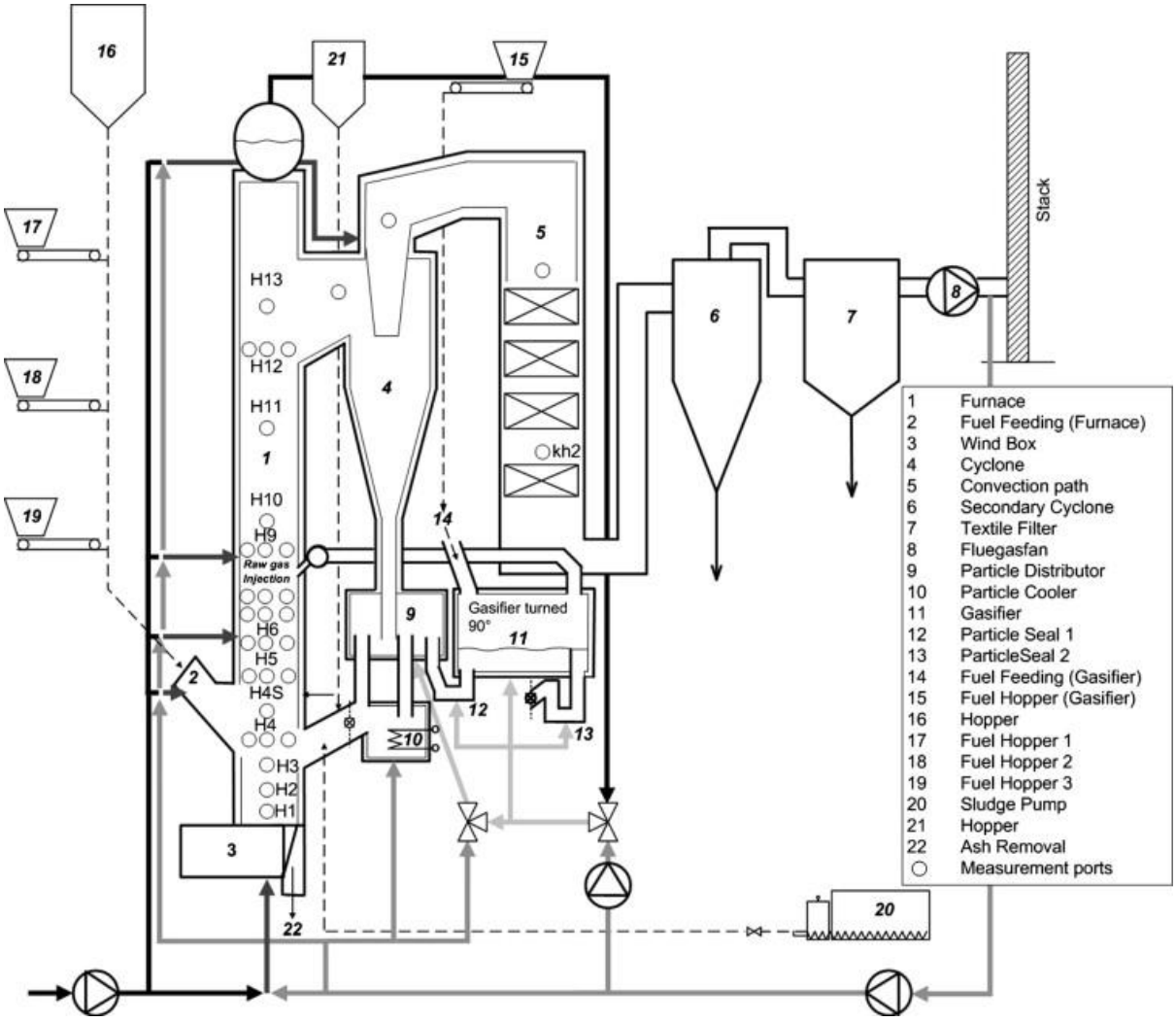

Figure 1. The layout of the Chalmers 12MW biomass boiler and combined 2-4MW gasifier. Bed material was extracted from a port between H2 and H3 in the central furnace[2].

Material characterization

SEM-EDX (Scanning Electron Microscopy equipped with Energy Dispersive X-ray spectroscopy) was used as the primary tool to investigate particle structure and element interactions inside the particles. The SEM-EDX analysis was done with a FEI Quanta 200 FEG ESEM. Bed material was mounted in epoxy and polished so the cross-section of the particles was exposed and the inside of the particles could be investigated by SEM-EDX. The crystalline phases in the bed material were determined by powder X-Ray Diffraction (XRD). The XRD was a Brucker D8 ADVANCE equipped with a Cu Kα radiation source. The XRD spectrum was complemented with SEM-EDX. Elemental analysis was performed with ICP-SFMS according to ISO 17294-2:2016.

Using the method and fluidized bed batch reactor described in the section “determination of reactivity” phase changes during reduction and oxidation could be determined for the LD slag. Samples was extracted from the fluidized bed batch reactor after reduction without any final oxidation and compared to samples extracted after oxidation. Reduction was performed using syngas and steam according to the mixture described in Table 1. Here a 15 g LD slag sample was used and reduced for 60 s, same three times the time since three times the bed mass was used. The sample was exposed to inert N_2 during cooldown to prevent oxidation. This sample was then

investigated using XRD and compared to two oxidized samples that had been cooled down during oxidizing respective inert conditions as the normal reactivity tests.

The particle size distribution of the bed samples taken from the bottom of the boiler was analyzed. This was done with sieves ranging between the sizes of 45 µm to 500 µm. Attrition was further investigated using a jet-cup rig that enhances the attrition of the particles during a 60-minute period. The rig is formed so that a jet of air at about 100 m/s, under ambient conditions, is imposed on a 3-5 g sample that forms a vortex up to a settling chamber. In this settling chamber, the velocity goes down to ~0.005 m/s that allows particles >10 µm to fall and particles <10 µm to be captured in a filter. The attrition index, given in wt.%/h of loosed mass, was calculated for the time period 40-60 min. Further details of this rig can be found elsewhere[26]. The attrition test was performed on particles with a size range of 125-180 µm.

Bulk density was measured to investigate changes in the material. Bulk density was measured using the funnel method according to ISO 3923-1:2008. For these tests, the samples were first sieved to remove particles with a mesh size larger than 1.8 mm, which would otherwise get stuck in the measurement apparatus. The particles that were discarded were small stones and char particles that originated from the fuel.

Fresh LD-slag was investigated in a thermogravimetric analyzer (TGA) to determine weight changes during heat-up. The TGA was a TA-instruments of model Q500 connected to mass flow controllers to set atmospheric conditions for the sample. The samples were heated to the operating temperature of 850°C during inert condition, and then up to 950°C and back to 850°C. This was done to determine structural changes due to the increased temperature. After this cycling in inert, the atmosphere was changed to oxidizing conditions with 5% O_2 in N_2 to oxidize the sample followed by cooldown to room temperature.

It is expected that the Ca in the sample could be of importance during the reaction for several reasons, including increased catalytic activity, but also the ability to react with carbon dioxide in the gas. Quantification of CaO+$Ca(OH)_2$ was provided by leaching in of 1.0 g sample in 100 ml 10% sugar solution. The sample was ground and then leached for 25 min under constant stirring to provide sufficient time for CaO to react with the water to form $Ca(OH)_2$ and then dissolve into the water. Then the mixture was filtered and rinsed, the filtrate was titrated with 0.075M H_2SO_4. The acid consumption was then calculated to determine the total free calcium content as CaO-equivalents in the sample[27].

Determination of reactivity

To determine reactivity changes of the LD slag as a function of time operated in the 12 MW boiler extracted bed material was investigated in a laboratory batch reactor system as described in Figure 2. The reactor was constructed of quartz glass and had an inner diameter of 22 mm immersed in an electric furnace. Gas was distributed from the bottom of the reactor throw a pours plate where 15 g of bed material was placed. The material from the boiler was inserted without any further pretreatment. The temperature was measured in the bed via a K-type thermocouple enclosed in a quartz shell and the gas temperature was measured directly under the pours plate in a similar manner. Pressure fluctuation over the fluidized bed was measured between the top and bottom of the reactor. Pressure measurement was performed using a Honeywell pressure transducer with a frequency of 20 Hz, enough to monitor the pressure changes over the reactor due to fluidization of the bed material.

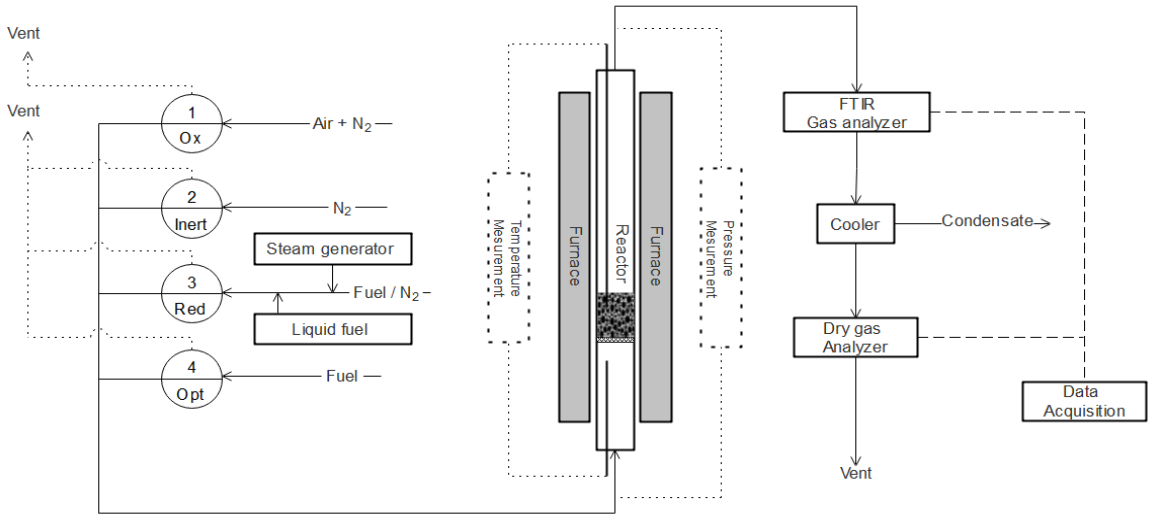

Figure 2. Schematic overview of the laboratory batch reactor system.

Gasses, steam and gas with the addition of liquid fuel were distributed to the reactor via heated tubes and automatic magnetic valves. Flows through the automatic magnetic valves was maintained by ventilation when closed to allow more stable flows and to reduce issues with condensation in the tubing. Steam was generated by injection of milli-q water into an evaporator at 150°C together with the fuel or N_2 gas.

Heat up of the equipment was performed in oxidizing conditions with 5% O_2 until stable temperatures and gas concentrations could be measured at 850°C. The bed material was exposed to oxidizing and reducing conditions in a cyclic manner at different temperatures, with intermediate inert flushes performed under 180 s with 1000 ml_N/min N_2. One cycle was made up of fully oxidized particles that were flushed with inert N_2 followed by a reduction, inert again to flush the reactor and ended with oxidation of the bed material until fully oxidized. The altering conditions of gases were used to simulate the conditions the bed material would be exposed to in both a CLC reactor and a regular CFB furnace, where both oxidizing and reducing zones are present. The oxidizing atmosphere was composed of a mixture of synthetic air and N_2 so that the total flow through the reactor was 1000 ml_N/min with a concentration of 5% O_2. The reducing gas was composed of 500 ml_N/min steam mixed with either syngas (50/50 CO/H_2 mixture), methane or benzene according to concentrations given in Table 1 to a total gas flow of 1000 ml_N/min. The benzene-N_2 mixture was obtained via bubbling of the gas throw a beaker containing benzene at room temperature and then cooled down to 6°C to reach a benzene stream with a concentration of 1.4 mol%. Benzene was used as a reference tar, hydrocarbons formed during gasification and combustion. The LD slag content of the bed material was 5 g for syngas and benzene cycles and 15 g for methane cycles. To obtain 15 g of bed material in the reactor silica sand with a size between 180 µm and 250 µm was added to the bed. The reason why only 5 g of slag was used for syngas and benzene experiments was due to that almost full conversion of the gases, at any temperature, was obtained with 15 g of LD slag, meaning that it should be difficult to establish a reactivity. Cooldown was performed after full oxidation in oxidizing conditions.

Before investigating the reactivity of the different bed samples, so-called activation cycles were performed. These cycles have been used in earlier study's regarding LD slag[24] and have also been shown to have an effect on the performance of other iron-based oxygen carriers, such as ilmenite[28]. Activation cycles, with reducing gas composition as described in Table 1, was performed until the conversion of CO was stable for the material, 3-8 cycles depending on the material. The experiments

with steam and a reducing component were performed three times at every temperature setting to confirm the repeatability of the results.

Table 1. Gas mixtures used for batch experiments.

Phase	Gas mixture	Gas flow [ml_N/min]	Temperature [°C]	Time [s]
Oxidizing	5% O_2, 95% N_2	1000	800-950	300-1200
Inert	100% N_2	1000	800-950	180
Reducing – Activation	100% 50/50 CO/H_2	900	850	20
Reducing – Syngas	50% Steam, 45% 50/50 CO/H_2, 5% N_2	1000	800-950	20
Reducing – Methane	50% Steam, 35% CH_4, 15% N_2	1000	800-950	20
Reducing – Benzene	50% Steam, 50% N_2 containing 1.4% Benzene, 20% N_2	1000	800-950	20

Gas analysis was performed on the hot gas from the laboratory reactor with a Thermo-Scientific IS50 Fourier transformed infrared (FTIR) analyzer. The gas cell in the FTIR and the connecting tubing was heated to 120°C to prevent condensation. The FTIR was calibrated for quantification of CO, CO_2, CH_4, H_2O, C_6H_6. Downstream from the FTIR, the off-gas from the furnace was cooled and condensate removed. The dry gas was then analyzed in a Rosemount NGA 2000 equipped with thermal conductivity and paramagnetic gas sensors for H_2 respective O_2. The NGA 2000 was also equipped with IR/UV sensors for CO, CO_2 and CH_4 as a reference for the FTIR.

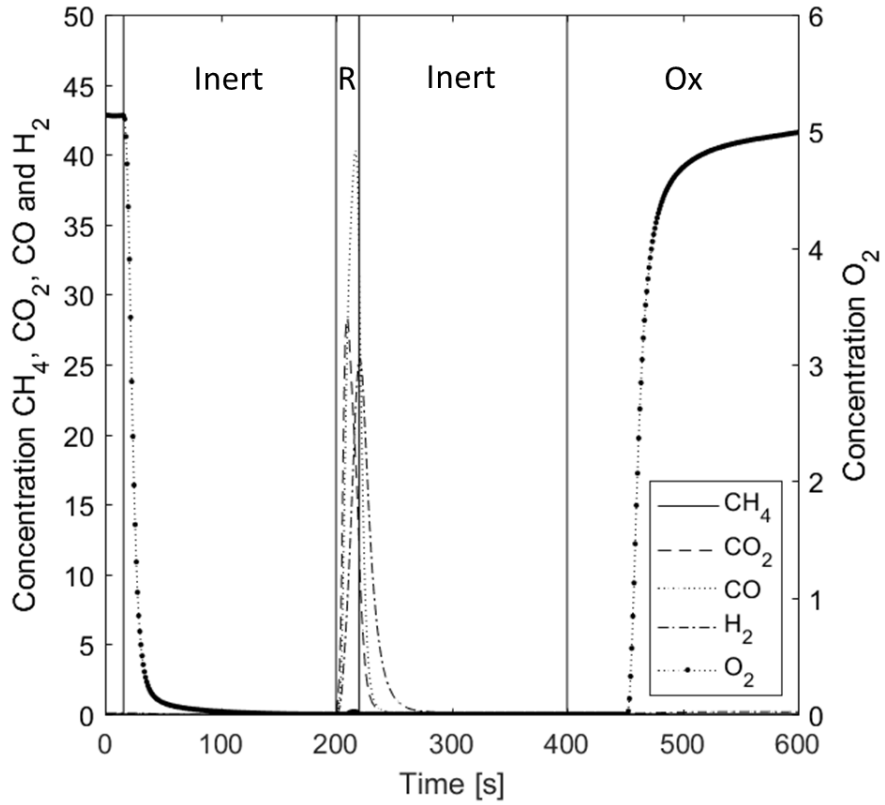

Figure 3. A dry-gas analysis of the gas composition for an entire red-ox-cycle with fresh LD slag that has been oxidized for 24h. The reducing phase is consisted of steam and syngas according to Table 1. Each cycle starts with an inert phase (inert) to flush the reactor with N_2, followed by a reducing phase (R). After reduction, the reactor is flushed again with N_2 and then an oxidizing phase (Ox) with diluted air to oxidize the particles is introduced.

Evaluation

The total conversion (γ) of C_6H_6, CH_4, CO and H_2 was based on the molar balance over the inflow and the outflow of respective gas. The concentration was determined from either the FTIR or NGA 2000 and the conversion of each fuel component was calculated according to equation (1).

$$\gamma_{Fuel} = \int_{t_{red}=0}^{t_{red}=end} \frac{x_{Fuel,in} * \dot{n}_{in} - x_{Fuel,out} * \dot{n}_{out}}{x_{Fuel,in} * \dot{n}_{in}} dt * 100\% \quad (1)$$

The molar outlet flow, $\dot{n}_{out}$, was calculated for the dry and wet gas flow from the gas composition in the measured outlet gas composition compared to the set composition in the inlet.

Oxygen uptake of the oxygen carrier, in this paper referred to as ω_{uptake}, was calculated from the oxidizing period of the experiments. Here, the oxygen reacting with the oxygen carrier could be calculated by comparing the outlet O_2 concentration profiles with a reference sample where no oxygen is expected to react, i.e. sand. Equation (2) was then used to calculate the total amount of oxygen transferred. The ω_{uptake} for the last of the activation cycle for each material was used as a guideline regarding oxygen capacity at 850°C after reduction with syngas.

$$\omega_{uptake} = \int_{t_{ox}=0}^{t_{ox}=end} \left(x_{O_2,ref} - x_{O_2,sample}\right) * \dot{n}_{out} \quad (2)$$

Results and Discussion

The fuel that was used in the boiler had an ash content of 0.5wt.% and the ash had a composition shown in Table 2. The ash was obtained at a temperature of 550°C, according to SS-EN-ISO 18122, and the analysis was performed using ICP-OES. The reference fuel in Table 2 is a mean value of 24 fuel ashes registered in Åbo Akademi chemical fractionation fuel database, techniques used to build this database can be found elsewhere[29]. Compared to the reference, the fuel used at the Chalmers boiler contained somewhat higher fractions of metals, Fe and Al, and some more silicon.

*Table 2. Elemental analysis of the fuel ash given in [wt.%]. The reference sample is based on a mean between 24 different wood chip fuels from Åbo Akademi Chemical Fractionation Fuel database. *Sulfur content is based on dry fuel content*

	Fe	Ca	Mg	Mn	Al	K	P	Si	S*
Fuel sample	0.66	23	3.8	1.5	0.53	12	1.3	1.7	<0.02
Reference	0.01	24	3.6	1.5	0.02	14	2.2	0.13	0.03

Material characteristics

From the elemental analysis of the bed materials, shown in Table 3, it can be observed that elements common in ash, such as K, P and S was accumulated in the bed. The ash dilutes the elements that are characteristics for LD slag, Fe, Ca, Mg and V. There is clearly alkali accumulation in the bed, although the degree of binding is lower compared to earlier studies with other materials[30]. However, more alkali was detected in the fly ash. It is clear from the vanadium content that the fly ash is rich in slag. The vanadium content in fuel ash is insignificant and the fly ash contains almost as much vanadium as the bed material. The sample names in upcoming figures and tables refer to the number of hours of full operation after startup that the particles had been inside the boiler under OCAC conditions.

*Table 3. Elemental analysis of the LD slag samples. Values are given in wt.%. *SC=Fly ash from Secondary Cyclone, **TX=fly ash from the textile filter, #: Ammonium sulfate was added to remove unconverted CO in the outlet of the cyclone.*

Sample Trend	Fe ↓	Ca ↓	Mg ↓	Mn ↓	Al -	V ↓	K ↑	P ↑	Si -	S ↑
As-received	17.07	31.73	5.88	2.64	0.76	1.51	0.05	0.25	5.61	0.10
Oxidized 24 h	16.09	30.52	5.40	2.45	0.74	1.54	0.04	0.23	5.42	0.11
OCAC 17 h	14.90	29.45	5.20	2.40	0.77	1.45	0.59	0.26	5.80	0.20
OCAC 41 h	13.50	27.30	4.86	2.19	0.69	1.42	0.95	0.29	5.14	0.29
OCAC 65 h	13.71	27.37	5.29	2.34	0.80	1.36	1.38	0.37	5.64	0.39
OCAC 68h +S	13.85	29.66	5.18	2.00	0.73	1.32	1.64	0.35	5.56	0.47
SC* OCAC 3h	15.39	27.02	5.79	2.38	0.90	1.37	0.49	0.23	5.70	0.13
SC* OCAC 64h	11.75	21.66	4.52	1.88	1.75	0.98	2.40	0.37	7.99	1.54#
TX OCAC 3h**	11.33	38.31	3.27	2.08	0.99	1.49	1.19	0.58	6.03	0.34
TX OCAC 64h**	7.48	23.23	3.28	1.52	0.52	0.99	7.69	0.79	2.86	6.57#

Compared to LD slag from other countries the Swedish LD slag contain much more vanadium[27,31,32]. With respect to the other major elements, this LD slag has similar amount of the different elements and could be seen as a representative of a typical LD slag [17]. Vanadium can act as an oxygen carrier[4], but since no phase or phase change of vanadium could be detected, it cannot be confirmed in this study.

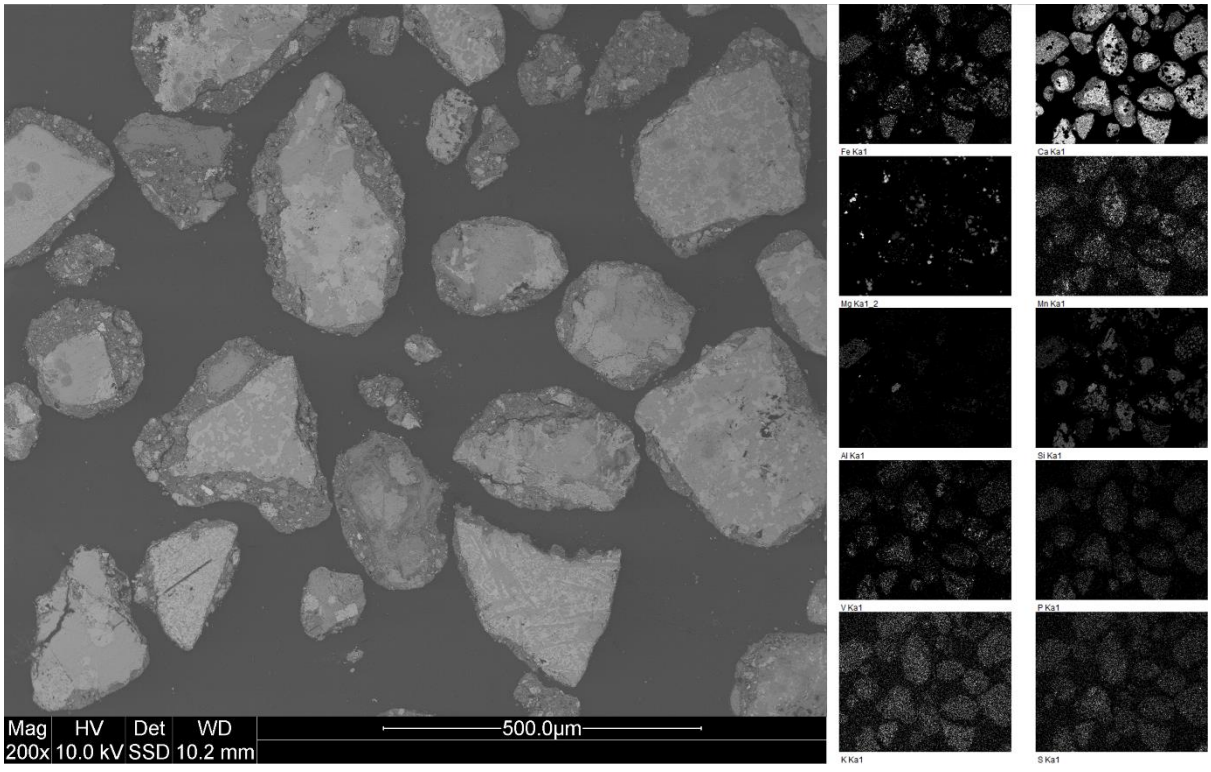

Figure 4. SEM-EDX of the cross-section of As-received LD slag particles.

From the SEM-EDX analysis of the different samples, it can be observed that LD-slag is, at least at a micro level, a very heterogeneous material. This can be seen in Figure 4 as the intensity of different elements Fe, Ca, Mg, Mn, Al, Si, V, P, K and S varies inside the particles. Each particle is unique regarding chemical distribution and structure. However, four common phases could be identified with SEM-EDX and these were also in conformity with phases identified with XRD in Table 4. These

four phases fit well with phases that have been suggested in other studies[27] and were more or less present in all samples:

1. A metal oxide phase containing mostly of iron, magnesium, manganese and some vanadium that is free from calcium. This phase corresponds to magnetite structure ($Fe_{3-x}A_xO_4$) including dopants were A=Mg and Mn.
2. A magnesium phase that consists of mainly magnesium iron oxide ($Mg_{1-x}Fe_xO$) and only minimal amounts of other metals. This phase was mostly located as small bubbles inside the slag particles.
3. A calcium phase also containing silicon and some of the transition metals in varying concentrations. According to the phases identified with XRD, the calcium phase consists of more or less pure calcium compounds such as lime (CaO), portlandite ($Ca(OH)_2$) and calcite ($CaCO_3$) as well as mixtures such as larnite (Ca_2SiO_3), hatrurite (Ca_3SiO_5) and srebrodolskite structure ($Ca_2Fe_{3-x}B_xO_5$) including dopants where B= Mg, Mn, Al and Si.
4. A silicon phase that also contains aluminum. The fourth phase could not be identified with XRD, most likely due to the low concentration – even below 1 wt.% of aluminum in samples according to the elemental analysis given in Table 3.

Table 4. Phases that was identified with XRD for the different samples and the amount of $CaO+Ca(OH)_2$ that was quantified by leaching. $CaO+Ca(OH)_2$ is given as wt.% CaO-equivalents. A=Mg and Mn. B= Mg, Mn, Al and Si.

Sample	Detected phases	Free $CaO + Ca(OH)_2$ [wt.%]
As-received	$Mg_{1-x}Fe_xO$, $Ca_2Fe_{3-x}A_xO_5$, $(CaO)_xSiO_2$, $Ca(OH)_2$, $CaCO_3$, CaO	6.2±0.29
Oxidized 24 h	$Mg_{1-x}Fe_xO$, $Ca_2Fe_{3-x}A_xO_5$, $(CaO)_xSiO_2$, CaO	4.0±0.09
OCAC 17 h	$Mg_{1-x}Fe_xO$, $Fe_{3-x}A_xO_4$, $Ca_2Fe_{3-x}A_xO_5$, $(CaO)_xSiO_2$, CaO	3.4±0.09
OCAC 41 h	$Mg_{1-x}Fe_xO$, $Fe_{3-x}A_xO_4$, $Ca_2Fe_{3-x}A_xO_5$, $(CaO)_xSiO_2$, CaO	2.5±0.17
OCAC 65 h	$Mg_{1-x}Fe_xO$, $Fe_{3-x}A_xO_4$, $Ca_2Fe_{3-x}A_xO_5$, $(CaO)_xSiO_2$, CaO	2.6±0.07
OCAC 68h +S	$Mg_{1-x}Fe_xO$, $Fe_{3-x}A_xO_4$, $Ca_2Fe_{3-x}A_xO_5$, $(CaO)_xSiO_2$, CaO	2.6±0.09

Comparison of a sample of an LD slag sample that was reduced with syngas in the presence of steam and a sample that was oxidized after several cycles in the batch reactor was performed. XRD diffractograms showed a significant difference between these samples indicating which phases in the LD slag that have oxygen carrier potential. The oxygen release was related to a shift from magnetite ($Fe_{3-x}A_xO_4$) to wüstite ($Fe_{1-x}A_xO$) where A is dopants such as Mg and Mn where especially Mg is characteristic for the phase structure of wüstite.

Regarding the magnetite phase $Fe_{3-x}A_xO_4$, it could not be confirmed using XRD in the as-received sample or in the sample oxidized for 24 h. However, when the sample had been used in the laboratory batch reactor, it was observed that the XRD diffraction pattern was changed and was much more similar to the boiler samples. This suggests that the same phases that were stable in OCAC conditions may be stable in CLC conditions since the laboratory batch reactor operates more closely to CLC conditions, i.e. with a higher degree of oxygen transfer. Hence, the same underlying redox phenomena occur in both the OCAC boiler and in the laboratory fluidized bed, albeit likely at different time-scales.

Potassium originates almost exclusively from the fuel ash, see Tables 2 and 3. Analysis of the bed samples shows a time-dependent accumulation of potassium in the bed material. Furthermore, K seems to accumulate together in the silicon and aluminum phase in the used samples, as determined by the SEM-EDX analysis of different samples. This could indicate that potassium binds up in the compound of $KAlSiO_4$ and other similar potassium aluminum silicates compounds that have been suggested in other studies [22]. However, no phase with this mixture could be confirmed with XRD. Higher concentrations of alkali such as potassium were found, as expected, in the secondary cyclone and textile filter (fly ash) compared to the bed material after >60h operation. It was expected since issues with CO emissions from the boiler during the operation was detected and could be associated with the inhibiting effects of potassium on combustion[33,34]. The CO emissions were decreased when both ammonium sulfate and elemental sulfur was introduced to the cyclone leg and the bottom bed respectively, two different methods to introduce sulfur for decreased corrosion due to alkali (KCl)[29,35] and obtaining a higher conversion of CO.

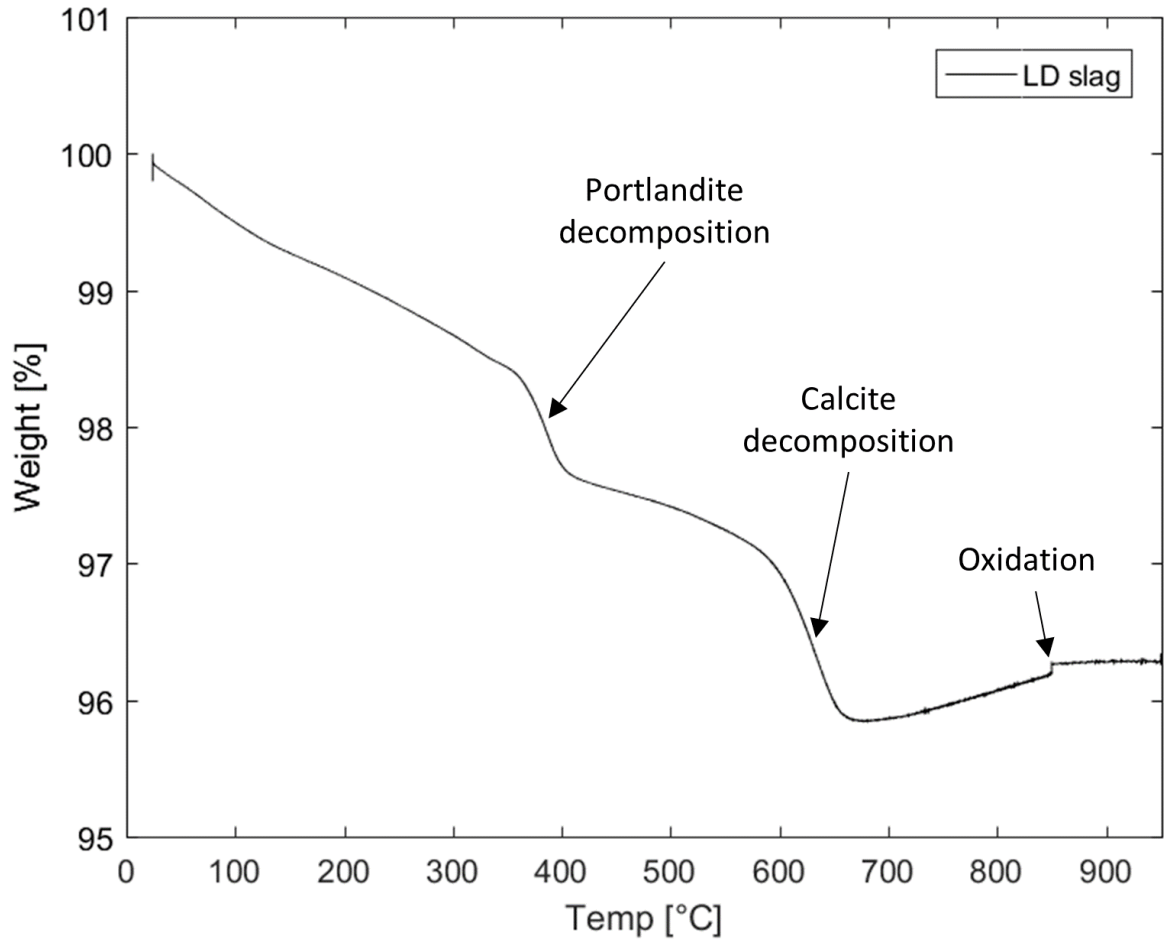

Figure 5. TGA of as-received LD slag sample weight change as a function of time during heat-up in inert atmosphere with a ramp of 2°C/min followed by oxidation with 5% O_2 in N_2. Decomposition reactions occur at similar temperatures as earlier studies[27].

From the phases identified by XRD given in Table 4, it can be noticed that all samples used in the boiler were similar with no significant changes in crystal structure. Fresh as-received LD slag was characterized by its free calcium phases, portlandite ($Ca(OH)_2$ like components) and calcite ($CaCO_3$ like components). These are decomposed into CaO at elevated temperatures and then interacted to form other mixed phases, see Figure 5. The decomposition temperature is lower than for pure $Ca(OH)_2$ and $CaCO_3$ but similar too earlier studies of LD slag samples[27] although with a greater weight

drop which indicates higher content of portlandite and calcite in this LD slag sample than reference. Comparing the observed free $CaO+Ca(OH)_2$ content between the as-received LD slag and the slag operated in the boiler, significantly higher concentrations was observed as can be seen in Table 4.

From the sieve tests performed on the LD slag extracted from the boiler, see Figure 6, some trends could be observed. Due to the high velocity of the air supply, small particles <100 µm of LD slag were removed in the primary cyclone. This could also be confirmed with detection of srebrodolskite, that is present in the LD slag, together with high levels of vanadium in the fly ash from the textile filter samples and secondary cyclone, see Table 3. Regarding agglomeration, a weak trend towards larger particle >500 µm as a function of time spent inside the boiler was observed. However, no agglomerates of particles could be found in any SEM investigations of the samples from the 12 MW_{th} boiler. The characteristics of these particles were that they were either char particles or small stones that most likely came from the fuel. There was also an increasing number of particles of ash melt that consisted mostly of silica, alkali and calcium with some minor amount of iron detected with SEM-EDX. These ash particles were not agglomerated with the LD-slag particles but rather a new fraction of porous particles of ash.

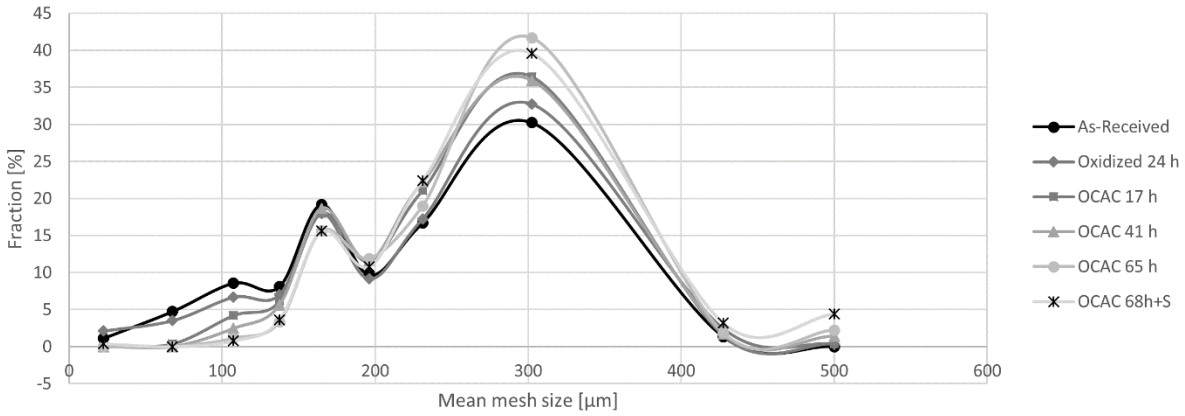

Figure 6. Sieve tests for the LD slag samples extracted during the operation in the 12MW_{th} CFB at Chalmers power central compared to fresh as-received and fresh slag that has been oxidized for 24h.

The bulk density of the particles, see Table 5, decreased considerably during the pretreatment of 24 hours of oxidation. This was due to loss of water bounded in portlandite and carbon dioxide decomposition of calcite. These reactions did not change the appearance of the particles but removed a considerable amount of mass. Regarding the operation of the boiler, the fine and low-density particles were lost to the secondary cyclone and textile filter. Therefore, a considerable increase in density was observed for the particles left in the boiler. During the operation, more and more porous ash particles and small stones appeared in the bed as mentioned above. This explains why the total density decreased for bed samples that had been operated for more than 41 hours in the boiler.

The attrition tests that were performed on particles with the size 125-180 µm showed a clear difference between the fresh samples compared to the samples from the boiler, see Table 5. The used samples had a relatively low linear attrition rate, which means that fragmentation of particles is limited and that the particles were relatively resistant to mechanical stresses. As-received and oxidized slag had a higher attrition rate and showed a logarithmical change as a function of time, see[26] for trends evaluation details. This suggests that the fresh material contains a relatively high number of structurally weak particles which are fragmented when introduced into the boiler as the result of mechanical stress. When comparing the as-received material internal structure to particles

processed in the boiler, as displayed in Figure 4 and Figure 7, it can be observed that as-received particles have a porous layer around the more solid internal that the used particles lack. No direct elemental composition Comparing to the large-scale boiler operation, the main bed material loss during the operation occurred in the beginning during the first 24 h. This was most likely due to a combination of drying of particles, decomposition reactions and loss of weaker particles.

From the reactivity tests performed in the laboratory fluidized bed batch reactor, it was observed that some particles agglomerated during test. This was observed by decreased pressure drop over the reactor and occurred during the heat-up of the system when the temperature reached 830-840°C. When the reactor was opened after the reactivity tests, it was also confirmed that some particles had agglomerated, this is referred to as "Severe" agglomeration in Table 5. However, with some particles, it was enough to just knock on the reactor during operation for detaching the agglomerates and obtaining normal pressure drop over the bed, thus indicating that the particles were fluidized. This is referred to as "weak" agglomeration in Table 5.

Table 5. Summary of measured bulk material properties of As-received LD slag and LD slag bed samples from the 12MW$_{th}$ boiler.

Sample	Bulk density [kg/m^3]	BET surface area [m^2/g]	Attrition [wt.%/h]	Oxygen carrier capacity/reactivity at 850°C [gO_2/100gOC]	Agglomeration	
					With sand	Without sand
As-received	1558	4.424	2.21	-	-	-
Oxidized 24 h	1405	0.997	2.16	0.91	Non	Non
OCAC 17 h	1715	0.415	0.66	1.02	Severe	Non
OCAC 41 h	1716	0.352	0.30	0.99	Severe	Weak
OCAC 65 h	1637	0.414	0.43	1.12	Severe	Weak
OCAC 68h +S	1639	0.521	0.54	1.16	Severe	Weak

It was observed, as can be seen in Table 5, that only the samples that had been operated in the boiler and with the addition of sand in the laboratory batch reactor showed severe agglomeration. Figure 7 shows SEM-EDX images of some of these agglomerates, where it can be observed that they are constructed of slag and sand particles. Potassium and silica form bridges, melted material, between the particles that form the agglomerates. It was also observed that this silicon-potassium melt only occurred between slag particles and sand particles, never sand-sand or slag-slag. This suggests that some potassium silicate is formed during solid-solid interaction between the slag particles and silica particle. Since the silica particles introduced to the laboratory batch reactor did not contain any alkali, the alkali must have diffused from the slag particles that in turn have absorbed some alkali from the fuel ashes.

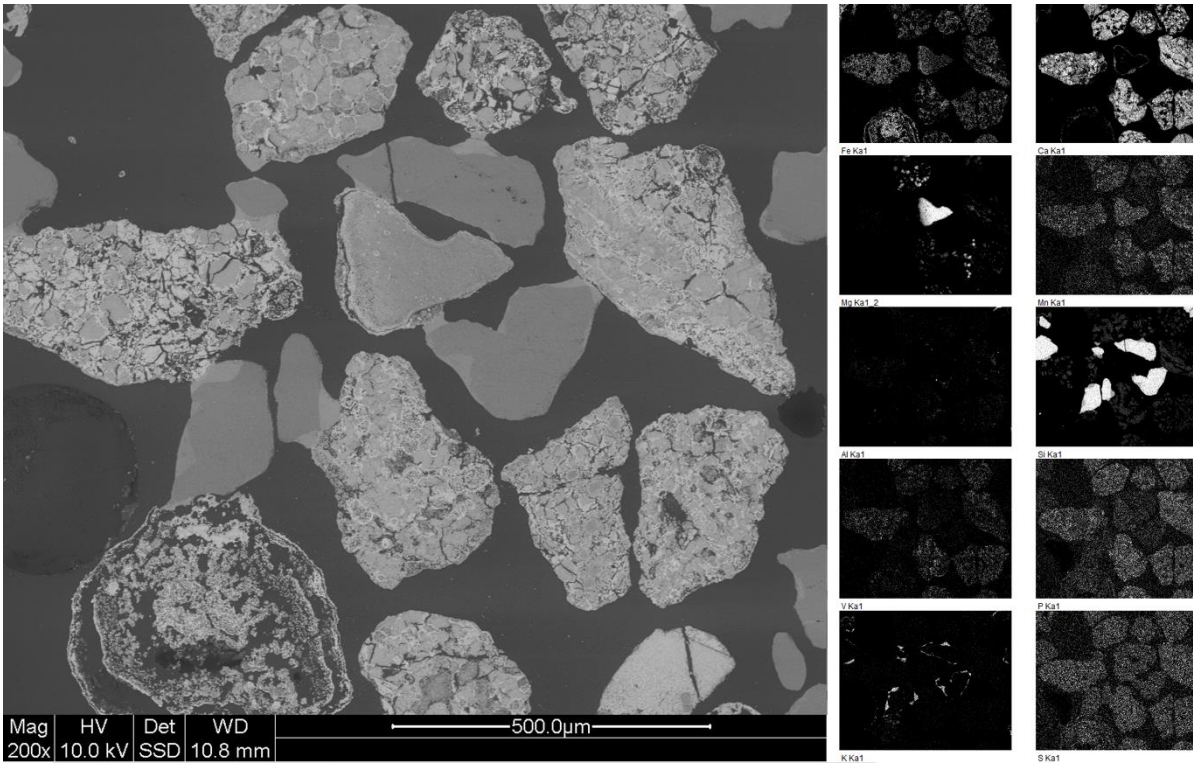

Figure 7. SEM-EDX on the cross-section of LD slag that has been operated 17h in the boiler and then tested in the laboratory batch reactor mixed with sand. The bridges between the particles contain mostly potassium and silicon that is the cause of the agglomeration.

Surface structural and chemical changes of the particles could be detected on the surface of the particles. Comparing as-received and oxidized LD slag to slag used in the boiler, the surface contained fines that are not present after the boiler, see Figure 8. In the as-received sample, the surface is more pours, see Figure 8 and Figure 4, this together with a large amount of fines contributes to the large surface area seen in Table 5.

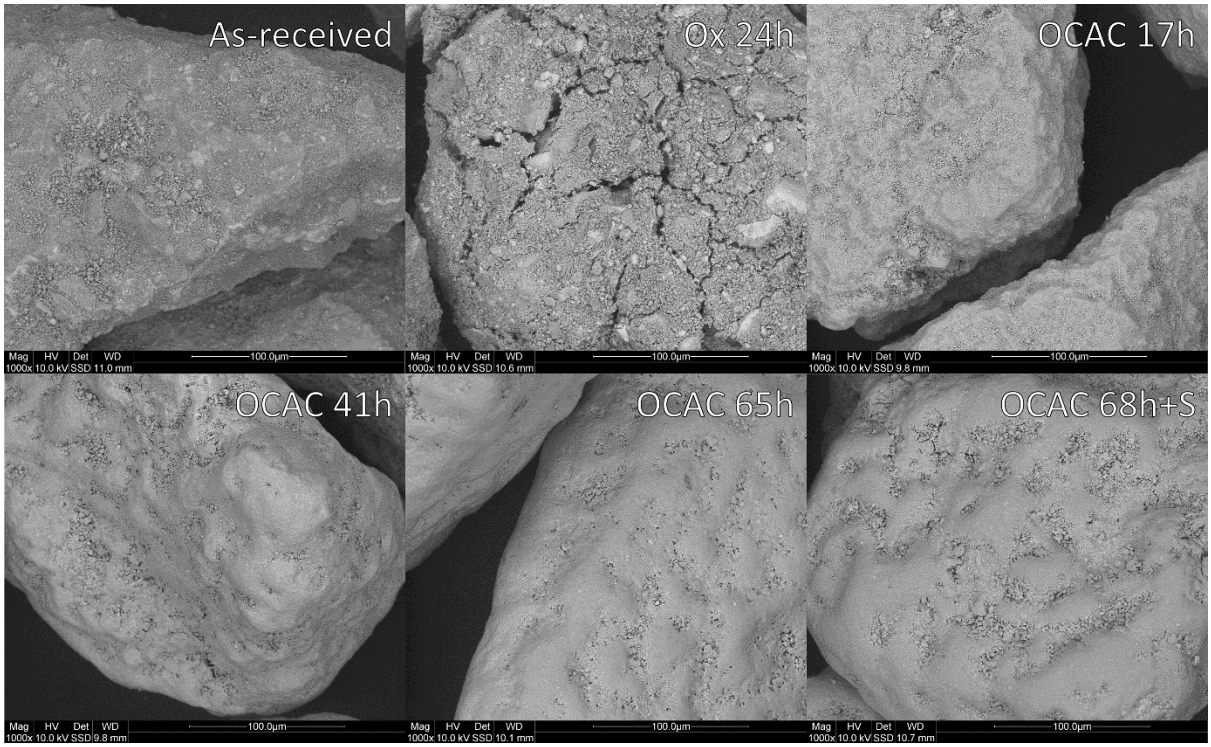

Figure 8. SEM images of particle surfaces from LD slag samples as-received, oxidized and extracted from boiler under OCAC conditions after 17, 41 ,65 and 68 hours. The three upper samples have a rougher surface with more small particles compared to the three lower samples.

From the image of the surface of the particles that have been operated for more than 41 hours some trends regarding ash deposits on the surface can be observed in Figure 8 and Figure 9. Accumulation of elements common is ash such as P, K and S were detected on the surface of the particles. Surprisingly, it was also observed that vanadium was accumulated on the surface of the particles, primarily together with P and K. Since there is no vanadium in the ash the vanadium has migrated towards the surface of the particles either due to the influence of ash or due to structural changes during combustion, as have been observed with iron when ilmenite have been used under OCAC conditions in the same boiler[30].

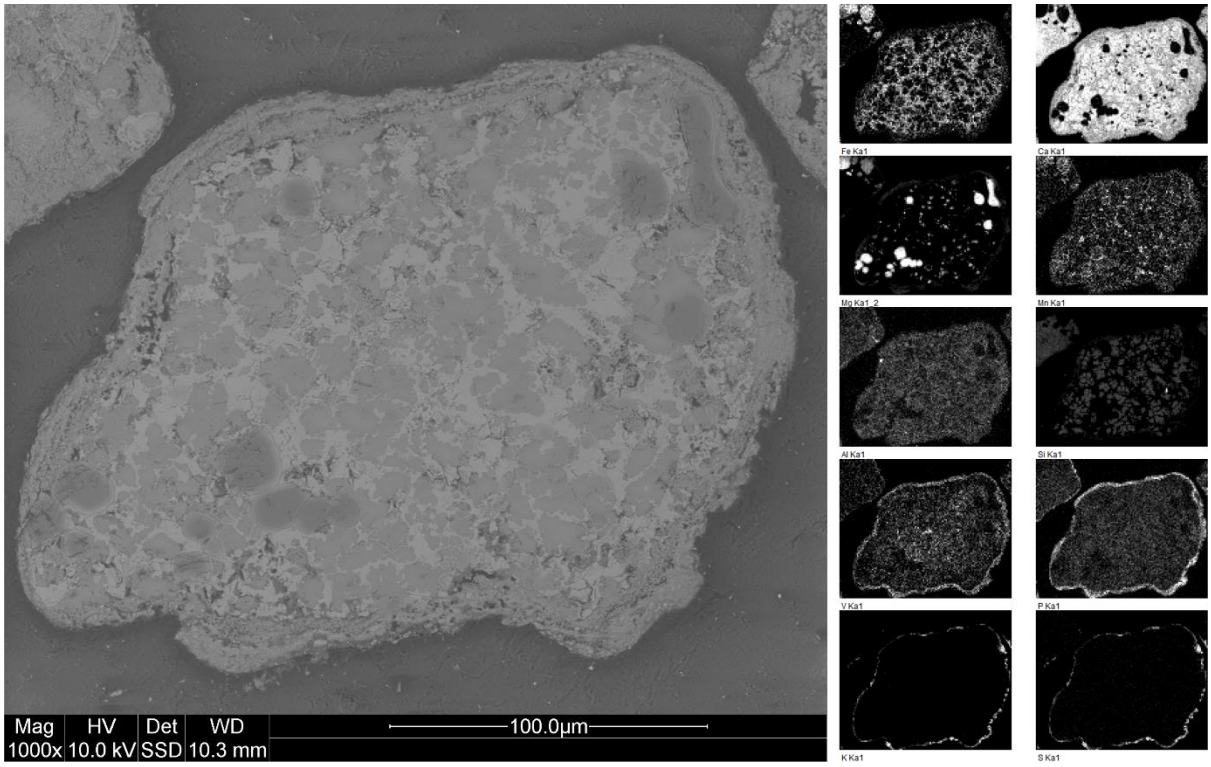

Figure 9. SEM-EDX on the cross-section of LD slag that has been operated 65h in the boiler. Accumulation of V, P, K and S can be observed on the surface of the particle.

Reactivity tests

The laboratory batch reactor tests that were performed on four LD slag bed samples extracted from the 12MW_{th} boiler at different operational times and compared with a fresh as-received sample that had been oxidized for 24h at 950°C. It should be mentioned that the samples were not sieved prior to testing, and thus the size distribution is that which is shown in Figure 6. However, clearly the distributions are very similar. Summaries of these reactivity tests are displayed in Figure 10, which show the conversion of the reactant gas as a function of temperature. The values given in the figures is a mean of the total conversion of the three cycles for the different fuels. The unused sample that had been oxidized for 24 h was used as a reference for the fresh sample. The degree of conversion for the LD slag that is free from ashes was relatively high regarding benzene and carbon monoxide compared to the conversion of methane. However, with increased ash content the conversion is decreased for all samples, although there is very little change for methane. Further, the carbon monoxide conversion for the sample that had been operated in the boiler for 17 h showed a higher degree of conversion compared to unused slag.

As expected, the conversion rate was increased when the test was performed at higher temperatures. Only the reaction with carbon monoxide was decreasing at 950°C. This is likely due to the fact that the water-gas-shift reaction is more shifted towards carbon monoxide and steam when the temperature is increased [25,36].

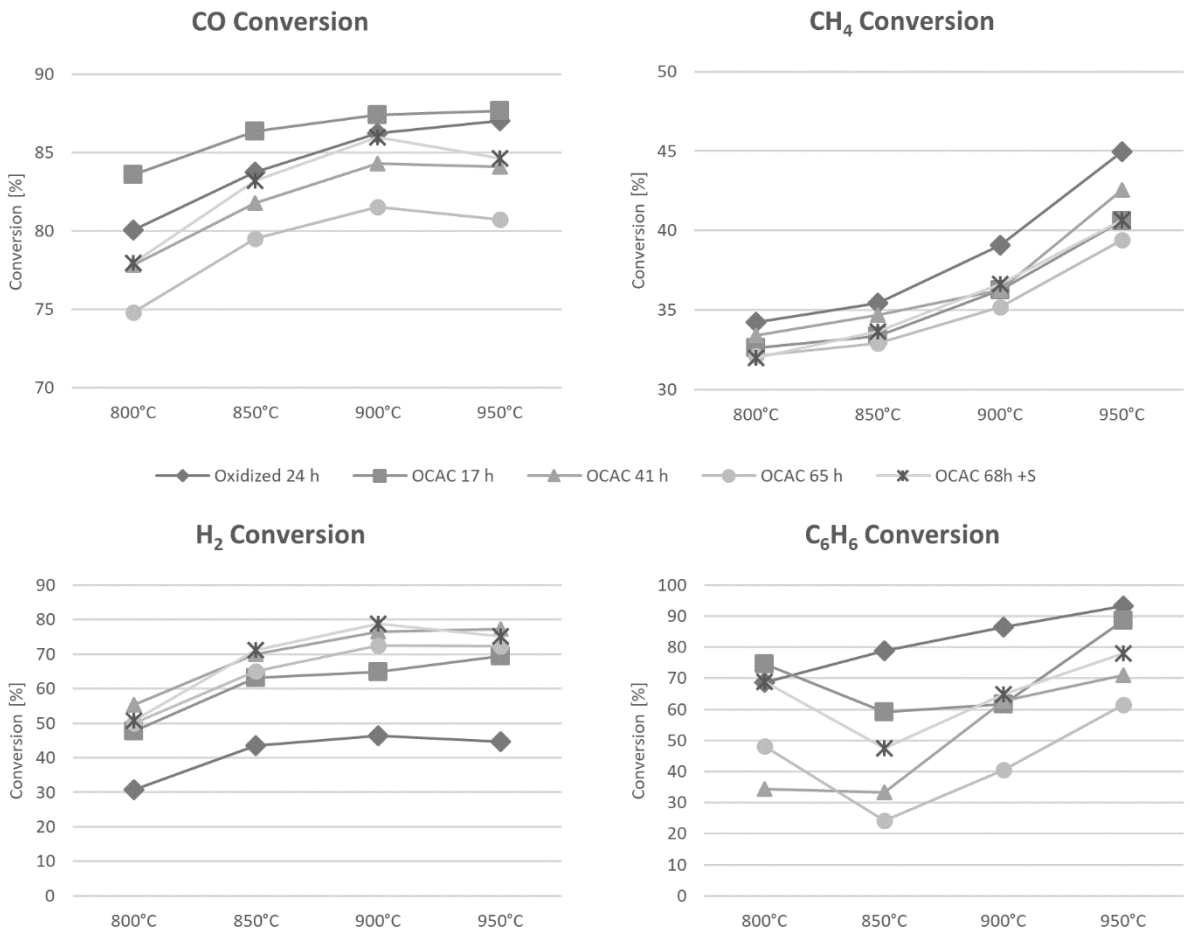

Figure 10. Four plots that describe the conversion of CO, H_2, CH_4 and C_6H_6 at temperatures between 800°C and 950°C in the batch reactor. CO and H_2 conversion were determined when syngas and steam were introduced to a sample of 5 gram of LD slag at different temperatures. C_6H_6 conversion was determined when a stream of nitrogen saturated with benzene was introduced to a sample of 5 gram of LD slag together with steam at different temperatures. CH_4 conversion was determined when methane and steam were introduced to a sample of 15 gram of LD slag at different temperatures.

Regarding the addition of elemental sulfur to the boiler bed, a difference can be seen in the reactivity. Reactivity towards syngas, methane and benzene was increased. This is most likely due to the inhibition of abundant alkali into sulfate compounds. Adding elemental sulfur or co-firing with fuel rich in sulfur, such as peat, are a common measure to prevent high-temperature corrosion by reduction of free alkali as well as KCl[29].

Conclusions

LD slag, a by-product from the steel manufactory, was used as an active bed material in Chalmers semi-commercial 12 MW_{th} CFB boiler operated with wood chips as fuel. The operation during a two-week period was successful, and the aim of this study was to evaluate how the oxygen carrier was affected by operation in the boiler during the first week. The effect of the time of operation on the bed material was studied by analyzing the chemical and mechanical properties of bed samples taken during the course of the operation, with a focus on the material from the bottom bed.

Overall, the conclusion of this study is that LD slag could be used as an active bed material with oxygen carrier properties. However, the mechanical and chemical characteristics do change as a function of operational time, which could be due to both ash interaction and internal particle changes. The lack of the ability to absorb a significant amount of alkali may be the most prominent

drawback with this type of oxygen carrier compared with other cheap materials for combustion processes [30]. This means that alkali will have a higher partial pressure in the boiler and downstream sections, compared to for instance ilmenite. However, the particles clearly maintained their redox behavior throughout the tests without any visible agglomeration, which can have many advantages with respect to boiler performance [2]

Regarding the properties of LD slag as an active bed material the following conclusions can be made:

- The major oxide phases identified in the oxygen carrier particles were very similar and independent of the operational time in the boiler or laboratory CLC batch reactor. The only exception was for the fresh sample, but which showed a transition to stable phases after redox testing the batch reactor.
- The oxygen carrier ability of LD slag originates from the reduction of Magnetite to Wüstite where dopants such as Mg and Mn are involved in the structures.
- After the loss of fine particles, the particle size distribution was more or less maintained during the operation of the boiler. This shows that there is a low tendency for agglomeration when ash is accumulated in the bed.
- Elements characteristic for fuel ash, such as potassium, sulfur and phosphorus were accumulated in the bed material. Potassium was absorbed to a low extent in areas rich in silicon and aluminum. Some ash was accumulated in the bed as separate particles.
- Reactivity towards syngas, methane and benzene decreased as a function of the operational time of the bed material in the boiler, although the degree of decrease depends upon the fuel, see Figure 10.
- Addition of elemental sulfur may have increased the reactivity of the used particle after 60h+ operation. However, the fresh material still displayed higher reactivity.

Acknowledgments

This work was financed by VR, Swedish Research Council (2015-04371), The Swedish Energy Agency (43220-1) and by Formas, the Swedish Research Council for Environment, Agricultural Sciences, and Spatial Planning.

The experimental campaign in the Chalmers Research boiler was made possible by close cooperation with SSAB Merox AB, which prepared and provided the LD slag particles, in addition to financial funding and expertize.

Referenses

1. IPCC. *Climate change 2014. Synthesis report. Climate Change 2014: Synthesis Report. Contribution of Working Groups I, II and III to the Fifth Assessment Report of the Intergovernmental Panel on Climate Change* (Gian-Kasper Plattner, 2014). doi:10.1017/CBO9781107415324

2. Thunman, H., Lind, F., Breitholtz, C., Berguerand, N. & Seemann, M. Using an oxygen-carrier as bed material for combustion of biomass in a 12-MWth circulating fluidized-bed boiler. *Fuel* **113,** 300–309 (2013).

3. Adánez, J. *et al.* Chemical looping combustion of solid fuels. *Progress in Energy and Combustion Science* (2018). doi:10.1016/j.pecs.2017.07.005

4. Hossain, M. M. & de Lasa, H. I. Chemical-looping combustion (CLC) for inherent CO2 separations—a review. *Chem. Eng. Sci.* **63,** 4433–4451 (2008).

5. Lyngfelt, A. & Leckner, B. A 1000 MWth boiler for chemical-looping combustion of solid fuels – Discussion of design and costs. *Appl. Energy* **157,** 475–487 (2015).

6. Steenari, B. M., Karlsson, L. G. & Lindqvist, O. Evaluation of the leaching characteristics of wood ash and the influence of ash agglomeration. *Biomass and Bioenergy* **16,** 119–136 (1999).

7. Elled, A. L., Åmand, L. E. & Steenari, B. M. Composition of agglomerates in fluidized bed reactors for thermochemical conversion of biomass and waste fuels: Experimental data in comparison with predictions by a thermodynamic equilibrium model. *Fuel* **111,** 696–708 (2013).

8. Knutsson, P. & Linderholm, C. Characterization of ilmenite used as oxygen carrier in a 100 kW chemical-looping combustor for solid fuels. *Appl. Energy* **157,** 368–373 (2015).

9. Adánez, J. *et al.* Selection of oxygen carriers for chemical-looping combustion. *Energy and Fuels* **18,** 371–377 (2004).

10. Lyngfelt, A. & Linderholm, C. Chemical-looping combustion of solid fuels - Technology overview and recent operational results in 100 kW unit. in *Energy Procedia* **63,** 98–112 (Elsevier, 2014).

11. Cho, P., Mattisson, T. & Lyngfelt, A. Comparison of iron-, nickel-, copper- and manganese-based oxygen carriers for chemical-looping combustion. *Fuel* **83,** 1215–1225 (2004).

12. Leion, H., Mattisson, T. & Lyngfelt, A. Solid fuels in chemical-looping combustion. *Int. J. Greenh. Gas Control* **2,** 180–193 (2008).

13. Leion, H., Mattisson, T. & Lyngfelt, A. Use of ores and industrial products as oxygen carriers in chemical-looping combustion. *Energy and Fuels* **23,** 2307–2315 (2009).

14. Jerndal, E. *et al.* Using Low-Cost Iron-Based Materials as Oxygen Carriers for Chemical Looping Combustion Chemical Looping -An Alternative Concept for Efficient and Clean Use of Fossil Resources La Boucle Chimique -Un concept alternatif pour un usage propre et efficace des . *Oil Gas Sci. Technol. – Rev. IFP Energies Nouv.* **66,** 235–248 (2011).

15. Ksepko, E. Sewage sludge ash as an alternative low-cost oxygen carrier for chemical looping combustion. in *Journal of Thermal Analysis and Calorimetry* **116,** 1395–1407 (Springer Netherlands, 2014).

16. Roudier, S., Sancho, L. D., Remus, R. & Aguado-Monsonet, M. *Best Available Techniques (BAT)*

Reference Document for Iron and Steel Production. *European Commission* (2013).

17. Chand, S., Paul, B. & Kumar, M. Sustainable Approaches for LD Slag Waste Management in Steel Industries: A Review. *Metallurgist* **60,** 116–128 (2016).

18. Yildirim, I. Z. & Prezzi, M. Chemical, Mineralogical, and Morphological Properties of Steel Slag. *Adv. Civ. Eng.* **2011,** 1–13 (2011).

19. Tossavainen, M. *et al.* Characteristics of steel slag under different cooling conditions. *Waste Manag.* **27,** 1335–1344 (2007).

20. Lundkvist, K., Brämming, M., Larsson, M. & Samuelsson, C. System analysis of slag utilisation from vanadium recovery in an integrated steel plant. *J. Clean. Prod.* **47,** 43–51 (2013).

21. Vachirapatama, N., Jirakiattikul, Y., Dicinoski, G., Townsend, A. T. & Haddad, P. R. Effect of vanadium on plant growth and its accumulation in plant tissues. *Songklanakarin J. Sci. Technol.* **33,** 255–261 (2011).

22. Mattisson, T., Li, Y., Hildor, F. & Linderholm, C. Use of cheap Mn- and Fe-based oxygen varriers in chemical-looping combustion (CLC) and gasification (CLG) with negative emissions of carbon dioxide. in May 22-24 (International Conference on Negative CO2 Emissions, 2018).

23. Keller, M., Leion, H., Mattisson, T. & Thunman, H. Investigation of natural and synthetic bed materials for their utilization in chemical looping reforming for tar elimination in biomass-derived gasification gas. *Energy and Fuels* **28,** 3833–3840 (2014).

24. Xu, L. *et al.* Performance of Industrial Residues as Low Cost Oxygen Carriers. in *Energy Procedia* **114,** 361–370 (Elsevier, 2017).

25. Schwebel, G. L., Leion, H. & Krumm, W. Comparison of natural ilmenites as oxygen carriers in chemical-looping combustion and influence of water gas shift reaction on gas composition. *Chem. Eng. Res. Des.* **90,** 1351–1360 (2012).

26. Rydén, M., Moldenhauer, P., Lindqvist, S., Mattisson, T. & Lyngfelt, A. Measuring attrition resistance of oxygen carrier particles for chemical looping combustion with a customized jet cup. *Powder Technol.* **256,** 75–86 (2014).

27. Waligora, J. *et al.* Chemical and mineralogical characterizations of LD converter steel slags: A multi-analytical techniques approach. *Mater. Charact.* **61,** 39–48 (2010).

28. Leion, H., Lyngfelt, A., Johansson, M., Jerndal, E. & Mattisson, T. The use of ilmenite as an oxygen carrier in chemical-looping combustion. *Chem. Eng. Res. Des.* **86,** 1017–1026 (2008).

29. Zevenhoven, M., Yrjas, P. & Hupa, M. 14 Ash-Forming Matter and Ash-Related Problems. in *Handbook of Combustion Vol.4: Solid Fuels* 493–531 (2010).

30. Corcoran, A. *et al.* Ash properties of ilmenite used as bed material for combustion of biomass in a circulating fluidized bed boiler. *Energy and Fuels* **28,** 7672–7679 (2014).

31. Monshi, A. & Asgarani, M. K. Producing portland cement from iron and steel slags and limestone. *Cem. Concr. Res.* **29,** 1373–1377 (1999).

32. Aarabi-Karasgani, M., Rashchi, F., Mostoufi, N. & Vahidi, E. Leaching of vanadium from LD converter slag using sulfuric acid. *Hydrometallurgy* **102,** 14–21 (2010).

33. Kassman, H., Normann, F. & Åmand, L.-E. The effect of oxygen and volatile combustibles on the sulphation of gaseous KCl. *Combust. Flame* **160,** 2231–2241 (2013).

34. Marinkovic, J., Thunman, H., Knutsson, P. & Seemann, M. Characteristics of olivine as a bed

material in an indirect biomass gasifier. *Chem. Eng. J.* **279,** 555–566 (2015).

35. Andersson, S. *et al.* Sulfur recirculation for increased electricity production in Waste-to-Energy plants. *Waste Manag.* **34,** 67–78 (2014).

36. Moe, J. M. Design of Water-Gas Shift Reactors. *Chem. Eng. Prog.* **58,** 33–36 (1962).